Radio Bright Structures near the Solar Poles at Millimeter Wavelengths

Silja POHJOLAINEN,[1,2] Fabrice PORTIER-FOZZANI, [3] and Delphine RAGAIGNE[4]

[1] *DASOP, Observatoire de Paris, Meudon, France*
[2] *Metsähovi Radio Observatory, Kylmälä, Finland*
E-mail: Silja.Pohjolainen@hut.fi
[3] *Equipe SOHO/EIT, Laboratoire d'Astronomie Spatiale, Marseille, France*
E-mail: fpf@astrsp-mrs.fr
[4] *DEA, Observatoire de Paris, Meudon, France*

Abstract

Polar radio brightenings have previously been observed in the wavelength range 15-48 GHz, but at higher frequencies the observations have not been so clear: besides local brightenings, also depressions and uniform brightness areas have been reported. In this study high frequency solar radio maps, observed at 87 GHz (3.5 mm) at the Metsähovi Radio Observatory, were analysed and compared with the SOHO/EIT EUV-images. The data consisted of nearly simultaneous radio and EIT maps observed during 1996 and 1997. Some radio enhancements were found to have polar plume bases, but most often the polar radio brightenings corresponded to coronal hole-like structures and bright diffuse sources seen in the EIT images. The radio depressions near the solar poles corresponded well with mini-coronal holes and coronal holes seen in EUV. However, only a few of the many – and sometimes large – low density regions seen in EUV were seen as depressions at millimeter waves. Therefore the conception of coronal hole brightenings can be extended to higher frequencies.

Key words: Sun: quiet — Sun: corona — Radio: Sun — EUV: Sun

1. Introduction

Radio brightenings near the solar poles were first analysed in the 1970's, after polar-cap brightenings had been observed at 13.5 and 8 mm with the Crimean 22-m telescope, see review in Kosugi et al. (1986). It has since become a well established fact that between 15 and 48 GHz the poles of the Sun seem brighter than the rest of the quiet Sun. At frequencies less than 15 GHz dark features are observed, probably due to the deficit of coronal material. At higher frequencies (from 85 to 105 GHz; the small frequency range is due to lack of observations and instruments available), uniform brightness as well as local brightenings and/or depressions have been reported.

Uniform brightness at microwaves and millimeter waves could be explained by similar chromospheric structure, as the emission has its origin deeper down in the solar atmosphere, in the upper chromosphere. However, when discussing polar brightenings one should bear in mind that they are based on a large variety of observations, ranging from very high latitude polar cap brightenings to individual 'polar sources' seen anywhere from about 40 degrees up to the poles. The polar cap brightenings have been connected with atmospheric structure (Hiei 1987) and observed or predicted limb brightening (Hiei 1987; Shibasaki 1997). The polar sources with enhanced radio emission have been connected with coronal hole brightenings (Brajša et al. 1996; Gary et al. 1997; Gopalswamy et al. 1997,1998) that could be caused by network features and unipolar magnetic fields (Kosugi et al. 1986; Gopalswamy et al. 1998), faculae (Riehokainen et al. 1998), plumes (Gopalswamy et al. 1992), and possibly even with the formation of fast solar wind (Gary et al. 1997; Gopalswamy et al. 1998).

Solar maps at millimeter wavelengths are rather rare: the Nobeyama 45-m telescope has sometimes been used for solar mapping at high frequencies (98 GHz - see Kosugi et al. 1986), the Nobeyama Radioheliograph works daily at 17 and 34 GHz, and the Metsähovi 14-m telescope is used for solar observations at intervals (within the antenna allocation schedules, see e.g. http://kurp-www.hut.fi/current/ant-schedule.shtml) at 37 and 87 GHz. After the Metsähovi antenna upgrade in 1992-1994, with the improvement of surface accuracy and adjustments made to the

Wavelength	Frequency	Temperature	Observation
3.5 mm	87 GHz	7200 K	upper chromosphere/corona

Wavelength	Ion	Temperature	Observation
304 Å	He II	8.0×10^4 K	chromospheric network
171 Å	Fe IX,X	1.3×10^6 K	transition region
195 Å	Fe XII	1.6×10^6 K	quiet corona
284 Å	Fe XV	2.0×10^6 K	active regions

Table 1.. Radio observations and EIT bandpasses

85-115 GHz tunable receiver, the millimeter wave solar radio maps have created growing interest. The possibility of comparing the data with the SOHO EIT-instrument made our data set start from April 1996.

2.   Observations

2.1.   Radio observations

The 14-m single dish antenna at Metsähovi gives 1.0 arc min spatial resolution (HPBW) at 87 GHz. The antenna was upgraded in 1992-1994, which made it better for high frequency observations. The maps are made by scanning the Sun in right ascension, by changing declination between scans. Fairly good temporal resolution is obtained by making "fast maps", i.e., the full solar disk is scanned in 9 minutes, see e.g. Urpo et al. (1997). The flux resolution in this study was estimated by using nearby tracking data. Track files are made by pointing the beam to a selected region on the solar disk and by measuring the flux density. The sampling rate in this mode is 20 samples per second. The noise level was determined from active region track files, which should give the maximum noise level as fluctuations in the active region itself are included. An alternative would be to track the sky and determine the noise level from there, but this is not a routine procedure during the observations. With this error analysis the flux resolution in the radio maps was determined to be between 0.3% and 0.5% of the quiet Sun flux, depending on the observing run in question. The variation is most probably instrumental and depends on the set-up at the given time. No absolute flux calibration is done during the Metsähovi observations, but the quiet Sun brightness temperature has previously been estimated (see e.g. Pohjolainen and Urpo, 1997) to be around 7200 K at 87 GHz, giving a brightness temperature resolution of 22—36 K for this study.

The solar maps that were analysed are "raw" maps, i.e., without any deconvolution methods applied. Because the beam is not sharp but more like a broad Gaussian with wings (sidelobes), an artificial limb darkening and an artificial sky brightening are observed near the true edge of the solar disk, see Lindsey and Roellig (1991). Because of the tilt in the solar B_0 angle we are still able to see up to 70 degrees towards the solar poles (at central meridian), but the view depends on the time of the year. For the near-limb sources to show up, deconvolution methods would be needed. We analysed here only those brightenings and depressions that were well outside this effect (i.e. well inside the solar disk). The exact shapes of these sources are still ambiguous without further knowledge of the beam profile, but on the other hand deconvolution can sometimes overestimate/underestimate the excess brightness temperatures.

Quiet Sun radio emission at 87 GHz (3.5 mm) originates from chromospheric heights – from a brightness temperature of about 7200 K – and it is mostly due to thermal bremsstrahlung. However, radio emission can be produced at greater heights if the plasma density and temperature are high enough in e.g., coronal loops. Also non-thermal emission mechanisms may be present.

2.2.   EUV observations

The Extreme Ultraviolet Imaging Telescope (EIT) onboard the *SOHO* spacecraft images the corona in four EUV wavelengths with a pixel resolution of 2.6 arcsec (Delaboudinière et al. 1996). From EUV lines – which represent different ion transitions – the chromosphere (He II), transition region (Fe IX/X) and corona (Fe XII, Fe XV) are imaged, see Table 1. Temperature diagnostics are made by wavelength ratios (Neumark et al. 1997), and 3-D coronal structure evolution is studied by comparing filter images (Portier-Fozzani et al. 1996).

2.3. Selection of data

We went through the radio maps measured at Metsähovi at 87 GHz (3.5 mm) in 1996 and 1997, and selected the ones that had close in time observations at one of the EUV wavelengths. In this way radio and EIT maps from 9 days were selected: April 12, 1996 (radio map at 13:57-14:05 UT), April 15, 1996 (radio at 12:05-12:13 UT), August 9, 1996 (radio at 07:23-07:32 UT), August 13, 1996 (radio at 12:31-12:39 UT), August 14, 1996 (radio at 12:55-13:03 UT), May 20, 1997 (radio at 13:03-13:12 UT), August 8, 1997 (radio at 11:30-11:39 UT), August 27, 1997 (radio at 12:13-12:22 UT), and August 28, 1997 (radio at 07:16-07:24 UT). The EIT Fe IX/X filter (171 Å) was mainly used to compare structures, as it is an intermediate temperature that shows well narrow shapes like loops. A lot more radio maps are available when nearness in time is not a requirement. In our position measurements the maximum time difference between a radio and an EUV map was 1.5 hours, but in that case more close-in-time observations were available at one of the other three EUV wavelengths.

In comparing features in radio and EUV one should be aware of the fact that the spatial resolution with a 14-m telescope at 87 GHz is rather poor, about 1 arcmin. This means that the true brightness is convolved with the beam, and therefore the given radio coordinates can be off the real source if the true brightness has complicated distribution within the beam. Also, a small bright point is not necessarily detected due to the dilution effect of the large radio beam. If sources looking similar in EUV are not both detected in radio, one must look for differences in temperature and/or density.

3. Observed features in millimetric radio and EUV

In the millimetric radio maps both radio brightenings and depressions could be seen. The radio brightenings were typically 0.5–1.5% (±0.3...0.5%) above the quiet Sun level (35–110 K if the quiet Sun is at 7200 K). The radio depressions were 0.5–2.0% below the quiet Sun level (corresponding to 35–145 K if quiet Sun at 7200 K). Sometimes diffuse brightness temperature enhancements (no peaks) were lying near the poles. With the articifial limb darkening effect we were not able to see further than 70 degrees towards the poles, at 0 longitude.

From the EIT images we were able to classify areas of different nature, mainly coronal holes, mini-coronal holes (small less dense regions), active regions, bright points, polar plumes, and diffuse structures that are generally thought to be non-resolved in the images.

As an example, a radio map from August 13th, 1996 and the corresponding SOHO EIT FeIX/X image are presented in Figure 1. The radio enhancements 2N and 3N near the solar north pole are clearly correlated to polar plumes in the EIT image, but for 1N the corresponding area could also be a bright point or an active region. The source 4N is a radio brightening, and 5N is a radio depression, that are located at coronal hole borders. In the southern hemisphere 1S and 2S are most probably active regions. The brightenings 3S and 4S, as well as the depression 6S, are connected to mini-coronal holes. The brightening 5S and the depression 7S are connected to bright diffuse sources.

To measure the uncertainties of position due to the different resolutions, we plotted the EIT image with resolution degraded to radio resolution (Figure 1). This confirmed that in some cases there is structural mixing and that the true locations of bright sources can be located nearby the peak intensities seen in the degraded image.

The temperature map derived from the EIT map on August 14, 1996 shows hot points and structures, presented in Figure 2. The radio map from the same day shows that some of the radio features are not only temperature dependent, but may be caused by density enhancements at lower/higher atmospheric heights (Figure 3).

4. Summary of statistical results

In the 9 radio maps observed at 87 GHz (3 mm) altogether 99 locations of radio features were determined. Of these 81 were brightness temperature enhancements and 18 were radio depressions (brightness below quiet Sun level). For 36 locations of brightness enhancement more than one EUV feature could be the counterpart. For the 45 radio bright locations where only one EUV feature could be identified within the radio beam area, the number of counterparts for the radio brightenings were the following:

- Active regions (9/45)

- Plume or plumes (3/45)

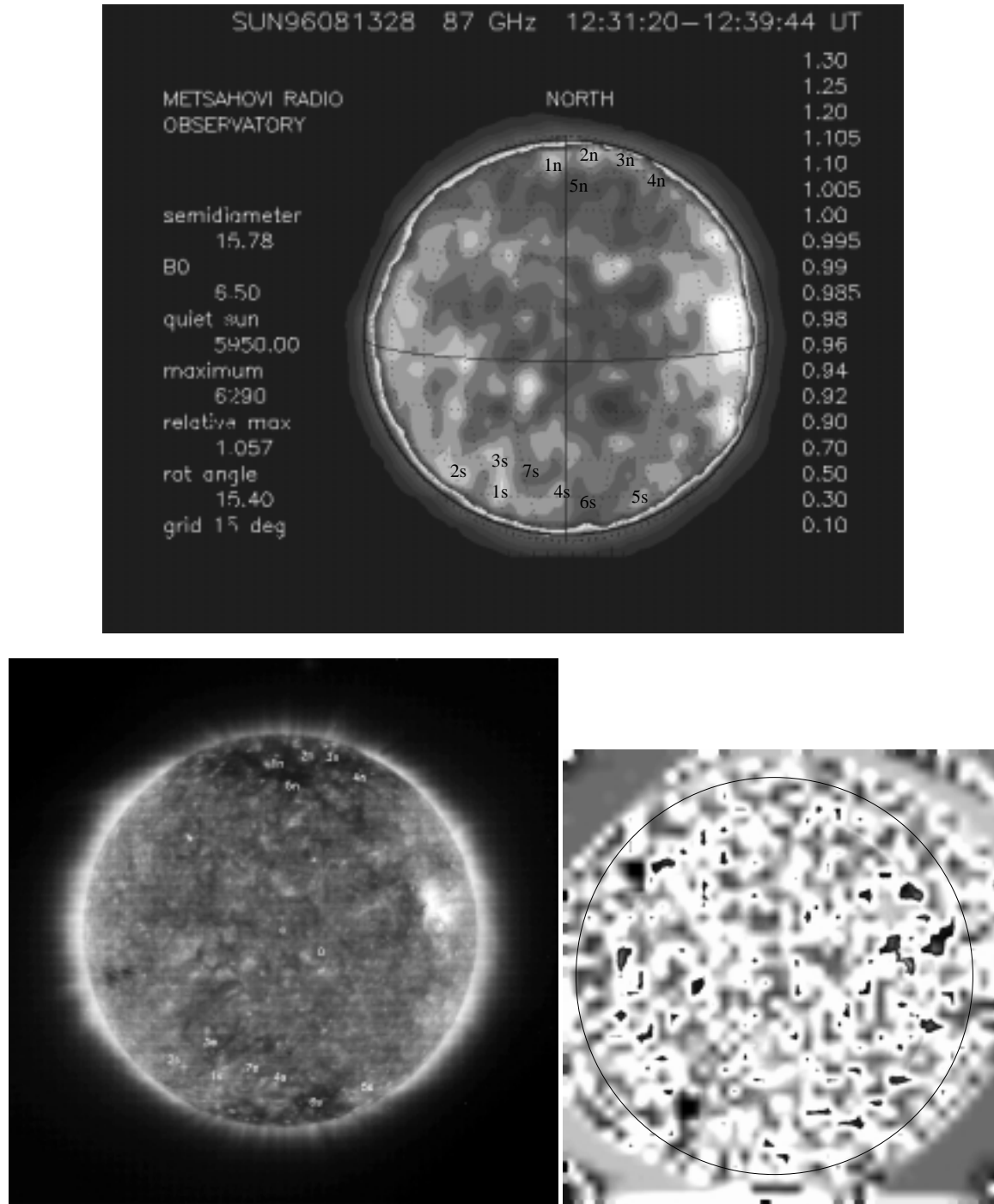- Diffuse bright structures (11/45)

Fig. 1.. Metsähovi solar radio map at 87 GHz (3.5 mm) from August 13th, 1996, at 12:31-12:39 UT (**top**), and SOHO/EIT Fe IX/X from August 13th, 1996, at 12:30:13 UT (**bottom left**). The correlated features are marked by numbers 1n...5n (northern hemisphere) and 1s...7s (southern hemisphere). See text for more detailed explanations on the sources. In **bottom right** is the EIT image with resolution degraded to radio resolution. The method was to do a mean average of the 2.6×2.6 arcsec^2 EIT pixels over 1×1 arcmin^2 radio resolution. A consequence of the method is a small dilatation, as is usual in that kind of imaging. The circle plotted over the image represents the new averaged limb position.
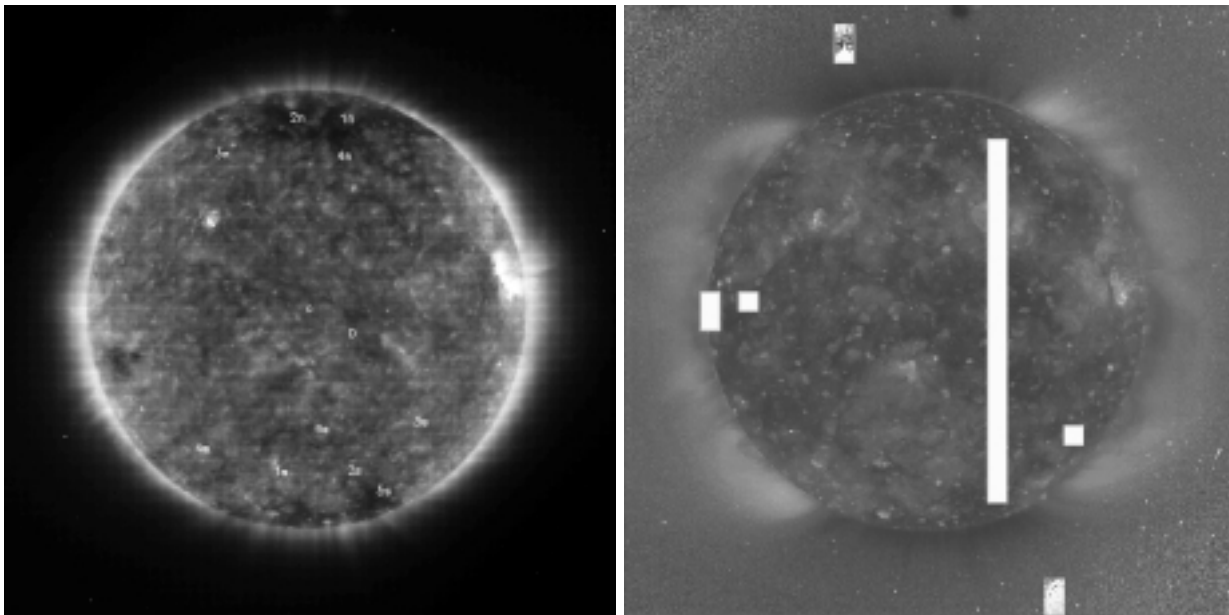
Fig. 2.. SOHO/EIT Fe IX/X image at 12:30 UT on August 14, 1996 (**left**). Temperatures derived from SOHO/EIT for August 14th, 1996 (between 0.8 – in black – and 1.6 MK – in white – except for the missing block due to low telemetry at that time) (**right**).
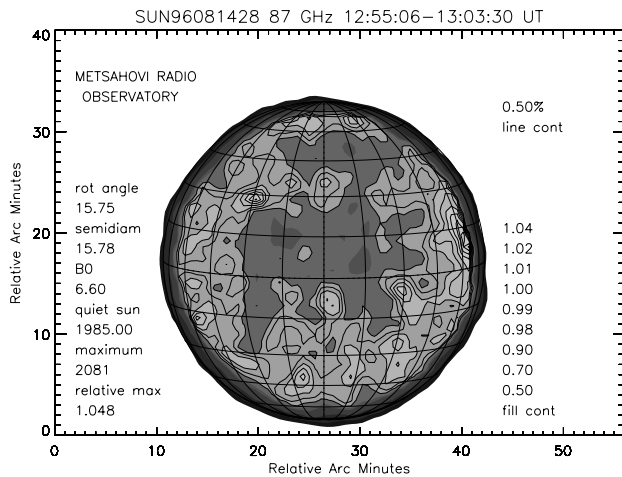

Fig. 3.. Metsähovi 87 GHz radio map at 12:55-13:03 UT on August 14th, 1996. The radio enhancements near the north pole were determined to have polar plume bases.

- Mini-coronal holes (13/45)

- Coronal holes (9/45)

The observed radio depressions (18 altogether) corresponded to:

- Mini-coronal holes (9/18)

- Coronal holes (2/18)

- Bright diffuse sources (2/18)

- A mixture of coronal hole/mini-coronal hole/border of coronal hole (5/18)

So the coronal holes seen in the EIT images corresponded to:

- Radio depressions (2)

- Radio enhancements (9),

and the EIT mini-coronal holes corresponded to:

- Radio depressions (9)

- Radio enhancements (13).

5. Discussion

We found that the millimeter wave radio depressions are very well correlated to coronal holes and other smaller less dense regions seen in EUV. We checked the locations of the radio depressions to see if there were any filaments present, but none were found – H_α dark filaments are known to cause radio depressions at mm-waves, see e.g. Vršnak et al., 1992. Low temperature filament plasma in the corona could also give signatures in the EUV emission, but we did not study this further.

Not all coronal holes or less dense regions looked as depressions in radio. In fact, the 'coronal hole brightening' can be stretched into millimeter waves by saying that some coronal holes look bright in radio and some not. This is in agreement with Gopalswamy et al. (1998), who suggest that only when enhanced magnetic flux is present in a predominantly unipolar region can radio enhancement (at microwaves) be seen. The SOHO EIT images analysed in this study did not show any features that could cause the brightenings at millimeter waves, but the magnetograms for these days are still to be analysed. Also the structures of polar plumes have to be studied in more detail, taking into account the possible differences (observed density, temperature) from line of sight variations.

The analysis presented here is in progress, and will be presented in a later paper. The analysis also has to take into account a possible selection effect because the radio features were selected first from the maps. Next step will be to reanalyse the data set by selecting the EIT features first. The difference of resolution between the two instruments is rather large, and by making an EIT image with the radio resolution we concluded that some artefact could be the result of structural mixing.

References

Brajša R., Pohjolainen S., Ruždjak V., Sakurai T., Urpo S., Vršnak B., Wöhl H. 1996, Sol. Phys. 163, 79
Delaboudinière J.-P. et al. 1996, Sol. Phys. 162, 291
Gary D.E., Enome S., Shibasaki K., Gurman J.B., Shine R.A. 1997, Bull. Am. Astron. Soc. 29, 8.01
Gopalswamy N., Schmahl E.J., Kundu M.R. 1992, Proc. First SOHO Workshop: Coronal Streamers, Coronal Loops, and Coronal and Solar Wind Composition, 113
Gopalswamy N., Shibasaki K., Thompson B.J., Gurman J., DeForest C. 1998, JGR, in press
Gopalswamy N., Thompson B.J., Shibasaki K. 1997, in K.S. Balasubramaniam, J. Harvey, and D. Rabin (eds.) Synoptic Solar Physics, ASP Conf. Ser. 140, 401
Hiei E. 1987, Publ. Astron. Soc. Japan 39, 937
Kosugi T., Ishiguro M., and Shibasaki K. 1986, Publ. Astron. Soc. Japan 38, 1
Lindsey C.A., Roellig T.L. 1991, ApJ 375, 414
Neumark J. et al. 1997, Am. Astron. Soc. Meeting 191, 73.07
Pohjolainen S., Urpo S. 1997, Fifth SOHO Workshop ESA SP-404, 619
Portier-Fozzani F., et al. 1996, PASP Conf. Ser. 111, 402
Riehokainen A., Urpo S., Valtaoja E. 1998, A&A 333, 741
Shibasaki K. 1997, in K.S. Balasubramaniam, J. Harvey, and D. Rabin (eds.) Synoptic Solar Physics, ASP Conf. Ser. 140, 373
Urpo S., Pohjolainen S., Heikkilä J., Wiik K. 1997, Solar Observations at Metsähovi in 1994-1995, Helsinki Univ. of Tech., Metsähovi Radio Res. Stat. Rep. 26
Vršnak B., Pohjolainen S., Urpo S., Teräsranta H., Brajša R., Ruždjak V., Mouradian Z., Jurač S. 1992, Solar Physics 137, 67